ORIGINAL ARTICLE

WILEY Xenotransplantation

Disabling of nephrogenesis in porcine embryos via CRISPR/Cas9-mediated *SIX1* and *SIX4* gene targeting

Junzheng Wang[1] | Manling Liu[1] (iD) | Lihua Zhao[1] | Yanru Li[1,2] | Manling Zhang[1,3] | Yong Jin[1,4] | Qiang Xiong[1] | Xiaorui Liu[1] | Lining Zhang[1] | Haibin Jiang[1] | Qiaoyu Chen[1] | Chenyu Wang[1] | Zhihuan You[1] | Haiyuan Yang[1,3] | Changchun Cao[4] | Yifan Dai[1,2,3] | Rongfeng Li[1,2,3]

[1]Jiangsu Key Laboratory of Xenotransplantation, Nanjing Medical University, Nanjing, China

[2]State Key Laboratory of Reproductive Medicine, Nanjing Medical University, Nanjing, China

[3]Key Laboratory of Targeted Intervention of Cardiovascular Disease, Collaborative Innovation Center for Cardiovascular Disease Translational Medicine, Nanjing Medical University, Nanjing, China

[4]Department of Nephrology, The Affiliated Sir Run Run Hospital, Nanjing Medical University, Nanjing, China

Correspondence
Rongfeng Li, State Key Laboratory of Reproductive Medicine, Jiangsu Key Laboratory of Xenotransplantation, Nanjing Medical University, Nanjing, China.
Email: lirongfeng@njmu.edu.cn

Abstract

SIX1 and *SIX4* genes play critical roles in kidney development. We evaluated the effect of these genes on pig kidney development by generating $SIX1^{-/-}$ and $SIX1^{-/-}/SIX4^{-/-}$ pig foetuses using CRISPR/Cas9 and somatic cell nuclear transfer. We obtained 3 $SIX1^{-/-}$ foetuses and 16 $SIX1^{-/-}/SIX4^{-/-}$ foetuses at different developmental stages. The $SIX1^{-/-}$ foetuses showed a migration block of the left kidney and a smaller size for both kidneys. The ureteric bud failed to form the normal branching and collecting system. Abnormal expressions of kidney development-related genes (downregulation of PAX2, PAX8, and BMP4 and upregulation of EYA1 and SALL1) were also observed in $SIX1^{-/-}$ foetal kidneys and confirmed in vitro in porcine kidney epithelial cells (PK15) following *SIX1* gene deletion. The $SIX1^{-/-}/SIX4^{-/-}$ foetuses exhibited more severe phenotypes, with most foetuses showing retarded development at early stages of gestation. The kidney developed only to the initial stage of metanephros formation. These results demonstrated that *SIX1* and *SIX4* are key genes for porcine metanephros development. The creation of kidney-deficient porcine foetuses provides a platform for generating human kidneys inside pigs using blastocyst complementation.

KEYWORDS
blastocyst complementation, CRISPR/Cas9, kidney development, pig, *SIX1*, *SIX4*

1 | INTRODUCTION

The number of patients with acute or chronic renal failure is rising each year, making kidney diseases a major worldwide problem.[1] At present, kidney transplantation is the only option for restoring all aspects of normal kidney function. However, the gap between the number of patients with end-stage organ failure and the number of available donor organs is rapidly expanding. One possible approach

to resolve the donor limitations is to use interspecies blastocyst complementation. This approach is based on emptying a "developmental organ niche" in one species by knocking out a specific gene or genes that are necessary for the formation of a particular organ and then using pluripotent stem cells (PSCs) from a different species to populate the empty niches and generate the desired organ.[2] The demonstration of the feasibility of intra- and interspecies blastocyst complementation using rodent models[3-5] now raises the intriguing possibility of generating human organs using easily accessible host animals, such as pigs, that are similar to humans in genetics, organ

J. Wang, M. Liu and L. Zhao authors contributed equally to this work.

size and physiology.[6] However, application of this principle for the generation of human organs first requires animal embryos, foetuses or neonates that lack the ability to generate the desired organs.

The development of the mammalian kidney includes three successive steps: pronephros, mesonephros and metanephros.[7,8] Kidney development begins with the formation of the nephric duct, also known as the Wolffian duct,[9,10] which grows caudally down the trunk and swells at the caudal region to form the ureteric bud (UB). The UB then outgrows and invades into the metanephric mesenchyme (MM).[11] The interactions between the UB and the MM include a series of reciprocal inductive events[12,13] in which the UB undergoes complex branching morphogenesis to give rise to the extra-renal ureter and the intra-renal collecting system,[14] while the MM condenses around the UB tips to form the cap mesenchyme.[15] This cap mesenchyme then undergoes a mesenchymal-epithelial transition (MET) to differentiate into the renal vesicles, comma-shaped body, S-shaped body and functional nephrons.[16] Consequently, the branching morphogenesis of the UB is a critical process in kidney development.

An intricate network of signals has been reported to control kidney development, with SIX-PAX-GDNF as the main signalling pathway regulating the mammalian metanephros genesis through a range of transcription factors including *SIX1*, *SIX4*, *PAX2*, *PAX8*, *GDNF* and *EYA1*. *SIX1* and *SIX4* belong to the murine homeobox *SIX* gene family, which is homologous to the Drosophila sine oculis (*SO*).[17] Studies on mice that lack *SIX1* have shown that these mice exhibit unilateral or bilateral renal hypoplasia because the UB grows out normally and elongates to differentiate into ureter but then fails to undergo branching morphogenesis.[18,19] *SIX1/SIX4*-deficient mice exhibit a more severely disrupted kidney phenotype when compared to *SIX1*-deficient mice, as the ureters and bilateral kidneys fail to develop. Mice lacking both *SIX1* and *SIX4* fail to form a detectable MM, and UB development is not induced.[20]

The nephric duct precursors show co-expression of the transcription factors *PAX2* and *PAX8*, members of the "paired box" (*PAX*) family of homeotic genes.[21] Deletion of *PAX2* results in mouse embryos that initially form the pro/mesonephros but lack both ureteric bud and mesenchyme, resulting in renal agenesis. The mutation of *PAX8* alone does not lead to any kidney abnormalities, but *PAX2/PAX8* double mutants fail to form the nephric duct.[22]

Another gene, *EYA1*, a homolog of Drosophila eyes absent, is initially expressed in the nephrogenic cord, caudal to the mesonephros, by the metanephric mesenchyme at embryonic day 11.5 (E11.5).[23] *EYA1* inactivation embryos do not form a morphologically distinct population of metanephric mesenchyme or a UB, which suggests that *EYA1* plays an important role during the conversion of nephrogenic cord cells into MM *SALL1* is a member of the multi-zinc finger transcription factors and is found in the MM. Its absence results in kidney agenesis caused by failure of UB invasion at E11.5.[24] Bmp signalling also plays a key role in UB branching.[25] BMP4 acts as a negative regulator of UB outgrowth and is expressed in the stromal mesenchymal cells that envelop the main trunk and the stalk of the branching ureters. *BMP4* null embryos die during early development.[26]

These genetic observations indicate that the up-stream regulators, *SIX1* and *SIX4*, might be good choices for establishment of a kidney-deficient pig model. However, the conservation of *SIX1* and *SIX4* is unknown across distantly related species, and the ability of disruption one or both of *SIX1* and *SIX4* genes to disable kidney development in pigs remains in question. Interestingly, the recent development of genome editing using clustered regulatory interspaced short palindromic repeats/CRISPR-associated protein (CRISPR/Cas9) technology and its combination with somatic cell nuclear transfer (SCNT) has allowed the creation of a number of useful pig models, thereby confirming that the CRISPR/Cas9-mediated genome editing system can be used effectively in pigs.[27] Similarly, the availability of porcine kidney PK15 epithelial cells, which have a wide range of applications in scientific research, including cell transfection,[28] virus infection[29] and vaccine production, makes them ideal candidates for investigating the signalling pathways of kidney development through in vitro experiments.

In the present study, we produced both $SIX1^{-/-}$ and $SIX1^{-/-}/SIX4^{-/-}$ porcine foetuses by combining the CRISPR/Cas9 system with SCNT technology and we also obtained $SIX1^{-/-}$ PK15 cell lines. We then investigated the functions of the *SIX1* and *SIX4* genes on the tissue and organ development of porcine foetuses, and especially kidney development. The effect of *SIX1* mutation on signal pathways of kidney development was also analysed. The study findings provide new insights into the function of the *SIX* gene family in porcine kidney development and reveal a possible strategy for the production of kidney-deficient pigs.

2 | MATERIALS AND METHODS

2.1 | CRISPR/Cas9 plasmid construction

The Cas9 expression construct pX330-U6-Chimeric-BB-CBh-hSpCas9 (Addgene plasmid 42230, Watertown, MA, USA) was a human codon-optimized SpCas9 and chimeric guide RNA expression plasmid. We used the online software (MIT CRISPR Design Tool: http://crispr.mit.edu) to design the sgRNA followed by the PAM sequence for targeting *SIX1* and *SIX4* genes. The sequences of sgRNAs are sgRNA1 (targeting *SIX1*): 5′-GCCATCGTTCGGCTTCACAC-3′ and sgRNA4 (targeting *SIX4*): 5′-AAGTGCGGCGGATATCAAGC-3′. The complementary oligos of the sgRNAs were synthesized, phosphorylated and annealed at 37°C for 30 minute, and at 95°C for 5 minute, followed by decreasing at 5°C/min to 25°C. The pX330-U6-Chimeric-BB-CBh-hSpCas9 plasmid was digested with BbsI and then ligated with the respective annealed oligos. The resulting CRISPR/Cas9 plasmids for targeting *SIX1* and *SIX4* were confirmed by sequencing.

2.2 | T7E1 cleavage assay

Porcine primary foetal fibroblast cells (PFFs) transfected with or without Cas9-sgRNA plasmids (as mentioned above) were cultured for 48 hour. Genomic DNA was extracted using a DNA extraction kit (TianGen, Beijing, China), and the genomic region spanning the CRISPR

target sites was PCR amplified. For sgRNA1, the forward primer was 5′-GGCCCGAAAAGCTGCGGAGTGAG-3′, and the reverse primer was 5′-TTGGGGTGGTTGTGAGGCGAGAA-3′. For sgRNA4, the forward primer was 5′-GACGAAGAAGGAGGAGTGAG-3′, and the reverse primer was 5′-GAAGTTCCGAGTGGAGTTGT-3′. The PCR conditions were as follows: 95°C for 5 minute, followed by 30 cycles of 95°C for 10 s, 60°C for 30 s and 72°C for 40 s, and a final 72°C for 7 minute. The T7E1 cleavage assay was performed using an EnGen® Mutation Detection kit (NEB, Beverly, MA) according to the manufacturer's protocol. Briefly, a total of 200 ng of the purified PCR product were mixed with NEB buffer 2, denatured and annealed to allow formation of heteroduplex using the following conditions: 95°C for 5 minute, 95°C to 85°C ramping at −2°C/s, 85°C to 25°C ramping at −0.1°C/s and 4°C hold. After reannealing, the products were digested with 1 μL of T7 endonuclease I at 37°C for 15 minute and then subjected to agarose gel electrophoresis. The cleavage bands were quantified with Image J (NIH, Bethesda, MD, USA).

2.3 | Cell culture, transfection and selection

Primary porcine foetal fibroblasts (PFFs) were derived from the skin of E35 Chinese Landrace pig foetuses. The PFFs were cultured in medium consisting of high glucose DMEM (Gibco, Grand Island, NY), 15% FBS (Gibco) and 1% penicillin/streptomycin solution (Gibco) at 37°C in 5% CO_2. Pairs of 1 μg targeting plasmids with 2 μg the neomycin-expression plasmid (pCMV-tdTomato) were co-transfected into 1×10^6 PFFs using a basic fibroblast nucleofection kit (VPI-1002; Amaxa Biosystems/ Lonza, Cologne, Germany) and nucleofection program U-023 following the manufacturer's protocols. After 24 hour of recovery, the electroporated cells were selected with 800 μg/mL of G418 (Gibco) in 10-cm dishes for about 10 days. Individual cell colonies were picked up and cultured in 24-well plates and then passaged to 12-well plates. Approximately 10% of the single colonies were lysed in NP-40 buffer at 55°C for 30 minute and then 95°C for 10 minute; the remaining cells were used for SCNT. The lysate was used as a template for PCR screening. The primers used in amplifying the target region were as follows. For the *SIX1* gene, forward: 5′-GGCCCGAAAAGCTGCGGAGTGAG-3′ and reverse: 5′-TTGGGGTGGTTGTGAGGCGAGAA-3′. For the *SIX4* gene, forward: 5′-CCCCACCGGGCAGATTGC-3′ and reverse: 5′-GCCAGGCGGTCCAGGTTG-3′. The PCR conditions were 95°C for 5 minute, followed by 35 cycles of 95°C for 10 s, 60°C for 30 s and 72°C for 40 s, and a finally 72°C for 7 minute. The PCR products were purified and then cloned into a pMD18-T vector (Takara Clontech, Tokyo, Japan) according to the manufacturer's instructions.

PK15 cells, purchased from iCell Bioscience Inc (Shanghai, China), were grown in MEM (Gibco) supplemented with 10% FBS (Gibco) and 1% penicillin/streptomycin solution (Gibco),and cultured at 37°C with 5% CO_2. The PK15 cells were seeded into 6-well plates (Corning Incorporated, Corning, NY, USA) 1 day prior to transfection at a density of 9×10^5 cells per well. The PK15 cells were then transfected with 8 μg *SIX1*-Cas9/sgRNA plasmids with 2 μg pCMV-tdTomato vector using Lipofectamine 2000 (Life Technologies, Carlsbad, CA, USA) according to the manufacturer's protocol. After a 24 hour

transfection, the cells were selected with 1000 μg/mL G418 in 10-cm dishes for 8 days. After G418 selection, resistant cell clones for each experimental group were pooled and collected. The genomic DNAs for different experimental groups were extracted and amplified by PCR for further sequencing assays.

2.4 | SCNT and production of mutant piglets

Methods used for porcine oocyte collection, in vitro maturation and SCNT were similar to our previously described protocols.[30] Briefly, the cumulus-oocyte complexes (COCs) were collected from ovaries and cultured for 42-44 hour at 38.5°C in an atmosphere of 5% CO_2 in air. The mature oocytes were enucleated as described by Dai et al,[31] and a single donor cell was then injected into the perivitelline space of the enucleated oocytes. Subsequently, the donor cell and recipient cytoplast were fused and activated to form reconstructed embryos. For the production of *SIX1* and *SIX1/SIX4* mutant foetuses, the reconstructed embryos cultured in PZM3 at 38.5°C for overnight or 2 days, respectively, and then transferred into the oviduct of an oestrus-synchronized recipient gilt Pregnancy status of the surrogates was confirmed by B-ultrasonic at 30 days after transplantation and monitored weekly thereafter. The foetuses were removed from the euthanized recipient gilts for dissection and sampling at different pregnant stages.

2.5 | Western blotting analysis

Kidney tissues from wild-type, $SIX1^{-/-}$ and $SIX1^{-/-}/SIX4^{-/-}$ foetuses were dissected, frozen immediately in liquid nitrogen and stored at −80°C until use. $SIX1^{-/-}$ cells and wild-type PK15 cells were collected by trypsinization and centrifugation. Total proteins from tissue and cells were extracted with RIPA lysis buffer (P0013B; Beyotime, Shanghai, China), and protein concentrations were measured by bicinchoninic acid assay protein assay kit (#23225; Thermo Fisher Scientific, Rockford, IL, USA) according to the manufacturer's protocol. Fifty micrograms of total proteins was used for SDS-polyacrylamide gel electrophoresis (SDS-PAGE), followed by transfer to polyvinylidene difluoride (PVDF) membranes (Merck Millipore, Bedford, MA). The membranes were blocked with 5% skim milk for 1 hour at room temperature and incubated overnight with primary antibody at 4°C, followed by incubation with secondary antibody for 1.5 hour at room temperature. The protein bands were detected with ECL Western blot detection reagents (CWbio, Jiangsu, China) according to the manufacturer's instructions. Western blotting data were quantified with Image J software. GAPDH served as the loading control. Primary antibodies used were anti-SIX1 polyclonal antibody (1:500; D4A8K, Cell Signaling Technology, Boston, MA, USA), anti-SIX4 (1:200; sc-390779; Santa Cruz, Dallas, TX, USA), anti-SALL1 (1:500; PP-K9814-00; R&D Systems, Minneapolis, MN, USA), anti-PAX2 (1:1000; ab79389; Abcam, Cambridge, MA, USA), anti-PAX8 (1:1000; ab191870; Abcam), anti-E-cadherin (1:1000; ab1416; Abcam) anti-BMP4 (1:200; sc-6896; Santa Cruz) and anti-EYA1 (1:1000; ab85009; Abcam). The secondary antibodies used were goat anti-rabbit antibody (1:2000; ab6721; Abcam) and goat anti-mouse antibody (1:2000; sc-2005; Santa Cruz).

2.6 | Histology and immunohistochemistry

Tissue samples obtained from the wild-type foetuses and knockout foetuses were prefixed with 4% paraformaldehyde overnight and then embedded in paraffin using standard procedures. Paraffin-embedded tissue samples were sectioned at 5 μm and mounted on glass slides. Sections were deparaffinized in xylene and rehydrated in a graded series of alcohol, followed by ddH$_2$O. The sections were then either stained with haematoxylin and eosin (HE) or immunochemically stained. Briefly, each section was incubated with primary antibody overnight at 4°C and with secondary antibody for 1 hour at room temperature. Primary antibodies were anti-SIX1 polyclonal antibody (1:200; D4A8K; Cell Signaling Technology), anti-PAX8 (1:200; ab191870; Abcam), anti-E-cadherin (1:200; ab1416; Abcam),anti-SALL1 (1:200; PP-K9814-00; RD Systems), anti-SIX2(1:200; 11562-1-AP; Proteintech, Wuhan, China), anti-EYA1 (1:200; ab85009; Abcam) and anti-BMP4 (1:200; sc-6896; Santa Cruz). The secondary antibodies were goat anti-rabbit antibody (1:1000; ab6721; Abcam) and goat anti-mouse antibody (1:1000; sc-2005; Santa Cruz). Micrographs were obtained using a Digital Sight DS-Ri1 camera attached to a Nikon Eclipse 80i microscope (Nikon, Tokyo, Japan) and semi-quantified by Image Pro Plus 6.0 (Media Cybernetics, MD, USA). The integrated optical density (IOD) of each micrograph was collected. Three fields for each slice (three slides per animal) were randomly selected for blinded measurements (n = 3 per group). The images were quantified using the immunoreactive area (IA) in μm^2 and the IOD. The staining intensity (SI) for each image was calculated as SI = IOD/IA, and the mean with standard deviation was obtained for each series.

2.7 | Off-target analysis

Potential off-target sites (OTSs) for sgRNA1 and sgRNA4 were predicted by using the CRISPR design tool (http://crispr.mit.
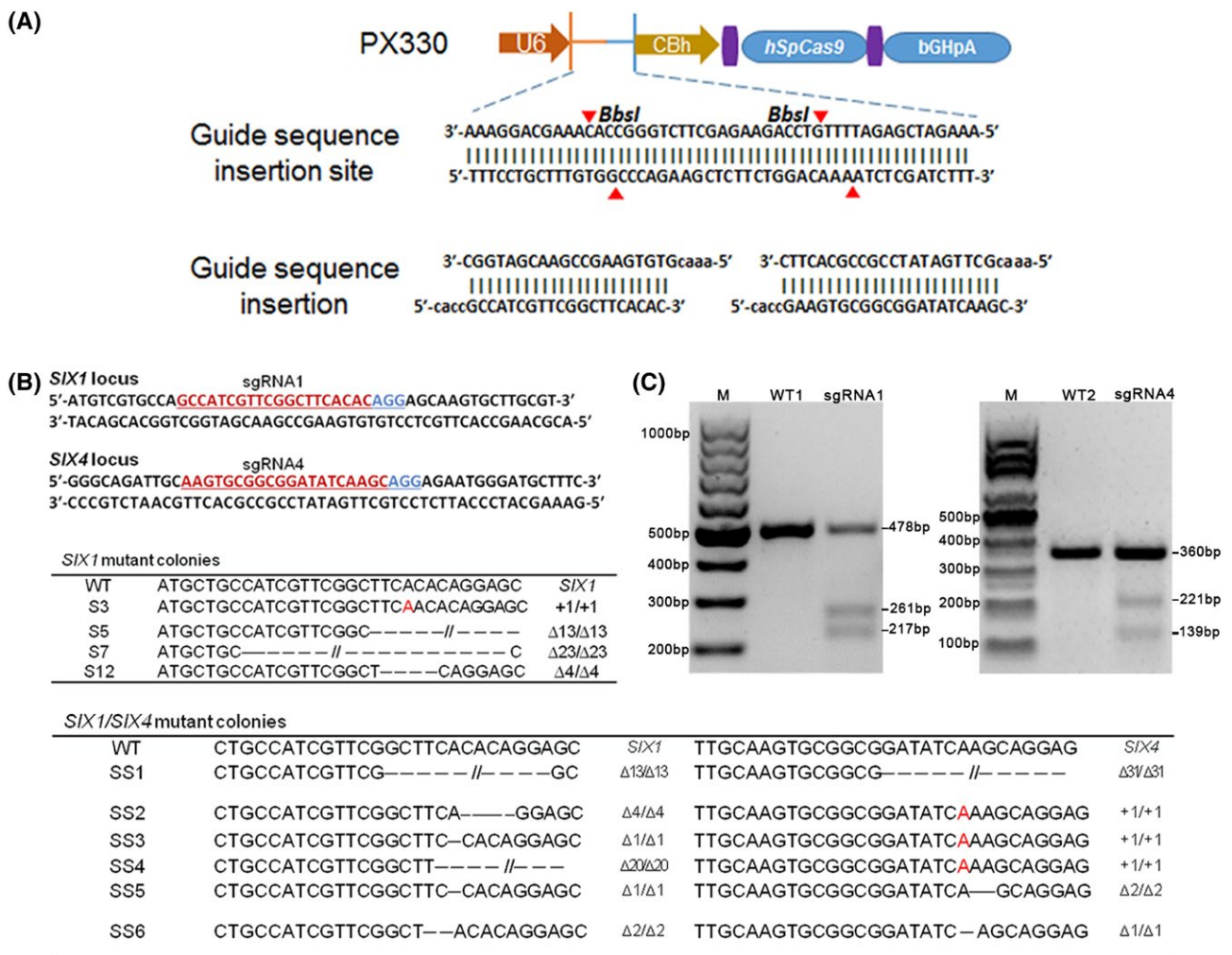

FIGURE 1 CRISPR/Cas9 mediates gene targeting in PFFs. A, Construction of recombination vectors. B, Schematic of sgRNAs targeting *SIX1* and *SIX4* loci. The target loci are located in the first exon following the start codon of these three genes. The sgRNA targeting sites are highlighted in red. PAM is highlighted in blue. C, T7E1 assay for CRISPR/Cas9-mediated cleavage at target site in PFFs. WT1 and WT2: PCR products of the wild-type PFFs treated with T7E1; sgRNA1 and sgRNA4: PCR products of PFFs transfected with Cas9/sgRNA1 and Cas9/sgRNA4 treated with T7E1; M: 100 bp DNA Ladder. D, Sanger sequencing of the targeting sites in mutant colonies used in SCNT. For each gene, the wild-type sequence is shown at the top. (+, insertion; Δ, deletion). PFFs, porcine foetal fibroblasts

edu/). The genomic regions flanking the OTSs were PCR amplified using genomic DNA isolated from *SIX1⁻/⁻* and *SIX1⁻/⁻/SIX4⁻/⁻* foetuses and WT controls. These PCR products were sequenced and aligned.

3 | RESULTS

3.1 | Generation of *SIX1⁻/⁻* and *SIX1⁻/⁻/SIX4⁻/⁻* pig foetuses

We disrupted the function of the *SIX1* and *SIX4* genes by choosing the first coding exon region of the two genes as the Cas9-sgRNA targeting site. The two sgRNAs targeting *SIX1* and *SIX4* genes were designed using online tools (http://crispr.mit.edu/) and cloned into the pX330 vector (Figure 1A). By assessing with the online tools,

the rating of *SIX1*-sgRNA was 91 and *SIX4*-sgRNA was 95. The target sites are shown in Figure 1B. We then tested the targeting efficiency of the Cas9-sgRNA plasmid by transfecting the Cas9-sgRNA vector into pig primary foetal fibroblasts (PFFs) and harvesting the genomic DNA after 48 hours. The PCR amplicons that spanned the *SIX1* or *SIX4* target site were treated with T7E1, and the cleavage bands showed that cas9-sgRNA targeting on the *SIX1* or *SIX4* gene was highly efficient; the mutation efficiencies of sgRNA1 and sgRNA4 were 48.5% and 26.9%, respectively (Figure 1C).

We established *SIX1* knockout cell lines by co-transfecting the Cas9-sgRNA1 vector and the TD-tomato plasmid into an early passage of primary PFFs derived from a 35-day-old male pig foetus, followed by selection with G418 for approximately 10 days and collected 23 single-cell-derived cell colonies. Genotyping analysis identified 18 *SIX1* homozygous/heterozygous biallelic mutant colonies
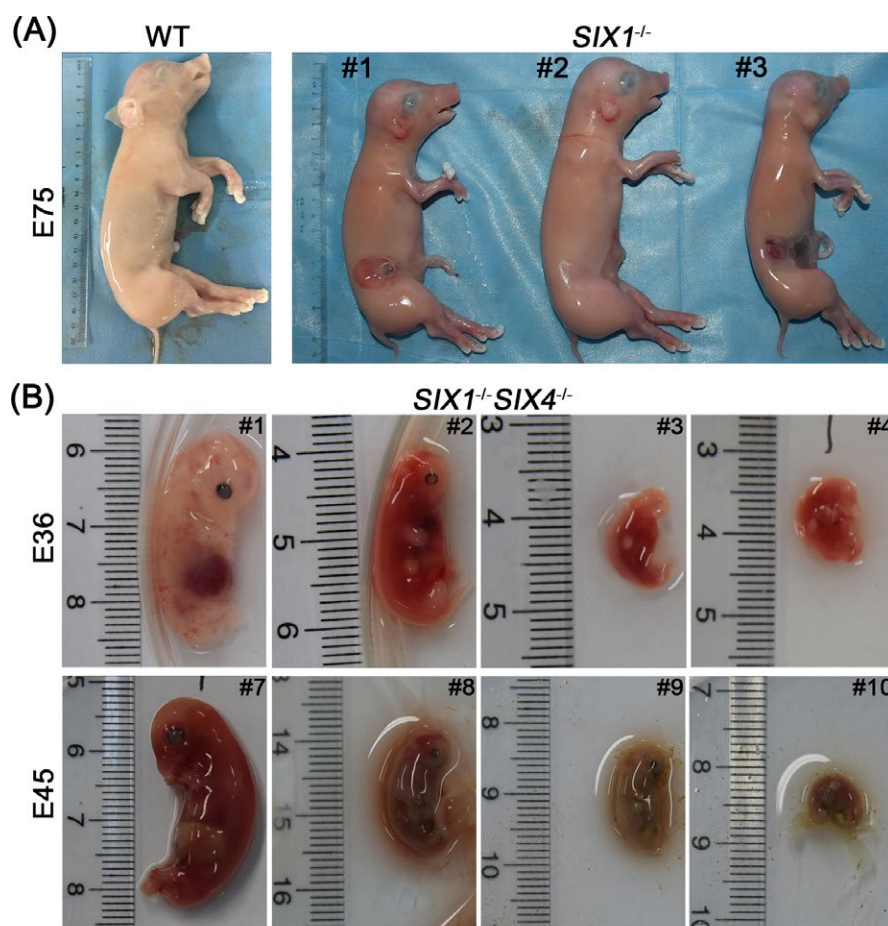

FIGURE 2 Generation of *SIX1⁻/⁻* pig foetuses and *SIX1⁻/⁻/SIX4⁻/⁻* pig foetuses via SCNT. A, Compared to the age-matched wild-type foetuses, *SIX1⁻/⁻* pig foetuses had a normal body shape and size. However, external developmental abnormalities were observed at the region of the kidney. B, Of the *SIX1⁻/⁻/SIX4⁻/⁻* pig foetuses, a few foetuses had a similar body size and appearance to the wild type, but most were significantly retarded in development at embryonic day 36 (E36) and all six foetuses at E45 showed dark colour and tended to degenerate. C, Genotypes of *SIX1⁻/⁻* and *SIX1⁻/⁻/SIX4⁻/⁻* foetuses and the corresponding cell colonies used for SCNT

SIX1⁻/⁻ foetuses	Genotypes	Colonies
SIX1⁻/⁻#1	SIX1:ATGCTGCCATCGTTCGGC-------------	S5
SIX1⁻/⁻#2	SIX1:ATGCTGCCATCGTTCGGCT----CAGGAGC	S12
SIX1⁻/⁻#3	SIX1:ATGCTGCCATCGTTCGGCTTCAACACAGGAGC	S3

SIX1⁻/⁻SIX4⁻/⁻ foetuses	Genotypes	Colonies
SIX1⁻/⁻SIX4⁻/⁻ #1 #2 #3 #4 #5 #6 #7 #8 #9#10#13#15#16	SIX1:CTGCCATCGTTCGGCTTC-CACAGGAGC SIX4:TTGCAAGTGCGGCGGATATCA---GCAGGAG	SS3
SIX1⁻/⁻SIX4⁻/⁻ #11#12#14	SIX1:CTGCCATCGTTCGGCTT –––//––– SIX4:TTGCAAGTGCGGCGGATATCAAAGCAGGAG	SS4

(Table S6). We used the same method to co-transfect the Cas9-sgRNA1 vector, Cas9-sgRNA4 vector and TD-tomato plasmid into PFFs to establish both *SIX1* and *SIX4* knockout cell populations. We picked up 18 single-cell-derived cell colonies for genotyping analysis, and 10 colonies were confirmed to be homozygous/heterozygous biallelic mutant colonies.

The *SIX1* and *SIX1/SIX4* homozygous biallelic knockout cell colonies were then chosen as donor cells for SCNT (Figure 1D). To generate *SIX1* knockout foetuses, a total of 1210 reconstructed embryos were transferred to three recipient gilts, and one of the three recipients was found to be pregnant (Table S5). Three foetuses were collected from the pregnant recipient pig at E75 by caesarean section surgery (Figure 2A). Genotype analysis showed that all three foetuses were biallelic *SIX1* gene mutants, corresponding to the mutant colonies (Figure 2C). At the morphological level, when compared to age-matched wild-type foetuses, these three foetuses had normal body shape and size. However, the #1 and #3 *SIX1*$^{-/-}$ foetuses had obvious abnormalities on the superficial skin tissue, and the kidney just was under the superficial tissue skin by necropsies.

A total of 1912 reconstructed embryos derived from *SIX1/SIX4* knockout cells were introduced into six recipient gilts; three gilts were found to be pregnant (Table S5). Our first attempt to retrieve an E75 foetus revealed only extremely degenerated foetal remnants. We therefore collected 10 foetuses at E45 (Figure 2B and Figure S3); one foetus had a similar body size to that of its wild-type counterparts, but the other foetuses showed significantly retarded development. All 10 foetuses showed an unusual dark colour and a tendency to degenerate when compared with their wild-type counterparts. Six foetuses were collected from a pregnant recipient pig at E36 (Figure 2B and Figure S3). A few of these foetuses had a similar body size and appearance to the wild type, but most were significantly retarded in development. However, none of the six foetuses showed the abnormal dark colour. DNA sequencing analysis results revealed that 16 foetuses were all *SIX1/SIX4* homozygous knockout mutants, corresponding to the mutant cell colonies (Figure 2C).

We determined the expression of *SIX1* and *SIX4* at the protein level in the gene edited foetuses and their wild-type counterparts by immunohistochemistry (IHC) and Western blotting. Unlike the expression in the wild-type controls, SIX1 protein was undetectable in the kidneys of the *SIX1*$^{-/-}$ pig foetuses (Figure 3A,B). Western blotting also confirmed the absence of both SIX1 and SIX4 protein in the *SIX1*$^{-/-}$/*SIX4*$^{-/-}$ pig foetuses (Figure 3C). Taken together, these results confirmed that authentic *SIX1*$^{-/-}$ and *SIX1*$^{-/-}$/*SIX4*$^{-/-}$ pig foetuses had been generated.

3.2 | Phenotypic characterization of *SIX1*$^{-/-}$ porcine foetus kidneys

Necropsy of the three *SIX1*$^{-/-}$ pig foetuses revealed that the kidneys of *SIX1*$^{-/-}$ Foetus #1 were smaller than the wild type and that *SIX1*$^{-/-}$ Foetus #2 had a unilateral kidney that did not migrate to the right position in the enterocoelia (Figure 4A). Comparison of the shape and size of the kidneys, hearts and spleens revealed that although the
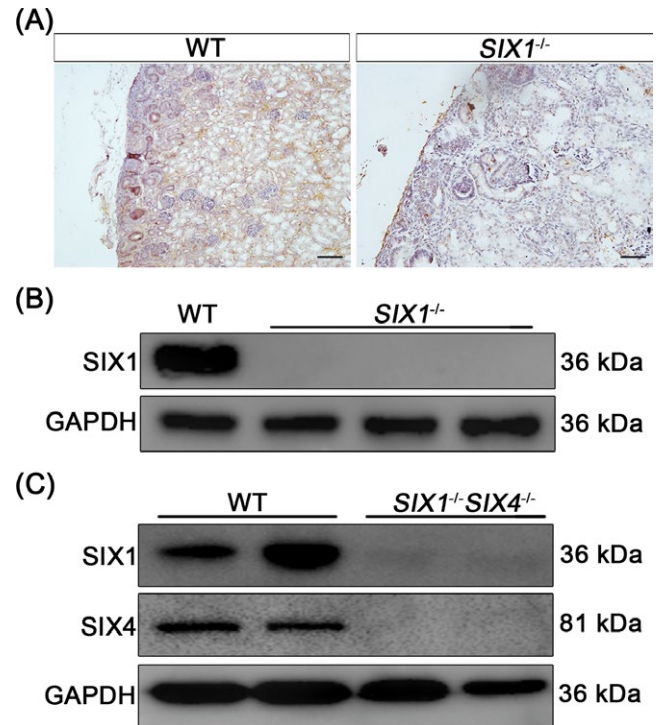

FIGURE 3 Immunohistochemistry and Western blot analysis of SIX1 and SIX4 protein in kidney. (A) Immunohistochemistry and (B) Western blot analysis of SIX1 demonstrated no detectable SIX1 protein in the kidneys of *SIX1*$^{-/-}$ porcine foetuses. (C) Western blot analyses of SIX1 and SIX4 protein demonstrated no detectable SIX1 and SIX4 protein in the kidneys of *SIX1*$^{-/-}$/*SIX4*$^{-/-}$ porcine foetuses. Bars = 100 μm

SIX1 mutant kidneys were significantly smaller than the wild type, no obvious differences were observed in their hearts and spleens when compared to the wild type (Figure 4B).

We also examined the kidneys for histologic abnormalities by HE staining of kidney sections from the porcine E75 *SIX1*$^{-/-}$ and wild-type foetuses. The developing kidney structures, such as glomeruli, tubules, comma-shaped body and S-shaped body, were present in both the *SIX1*$^{-/-}$ and wild-type porcine foetuses, indicating that the nephrogenic progenitors were able to undergo nephrogenesis in the *SIX1*$^{-/-}$ kidney. However, the nephrogenic zone was markedly widened in the *SIX1*$^{-/-}$ kidney, indicating a possible suppression of the process of MM differentiation (Figure 5A,B). The HE staining revealed that the renal tubules of the *SIX1*$^{-/-}$ kidney appeared to be undergoing vacuolar degeneration, whereas this phenomenon was not observed in the wild-type kidney (Figure 5C,D).

We also stained tissue sections with periodic acid-Schiff (PAS), Grocott's methenamine-silver (GMS), Congo red (CR) and Masson's trichrome to examine histologic changes in the glomerulus. We noted no significant differences between the *SIX1*$^{-/-}$ and the wild-type kidneys following PAS, GMS or CR staining, but Masson's trichrome staining revealed a significant increase in glomerular collagen fibres in the *SIX1*$^{-/-}$ kidney compared with the wild type, indicating that disruption of the *SIX1* gene could cause nephron damage (Figure 6). We also performed HE staining of the heart, liver, spleen and pancreas
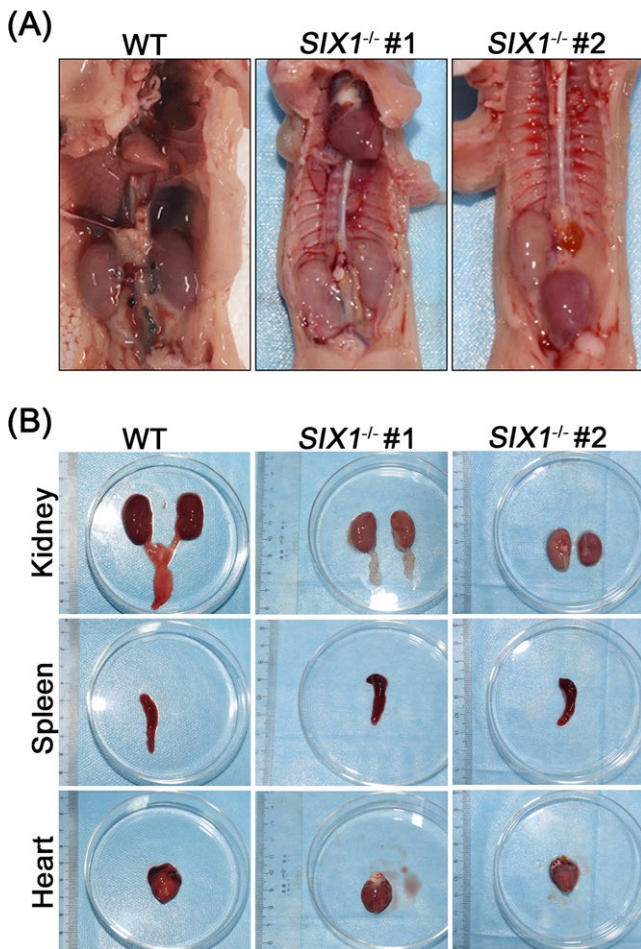
FIGURE 4 Phenotypic characterization of $SIX1^{-/-}$ porcine foetuses. (A) Necropsy findings of two of the three pig foetuses showed that $SIX1^{-/-}$ Foetus #1's kidneys were smaller and $SIX1^{-/-}$ Foetus #2's unilateral kidney did not migrate to the right position in the enterocoelia when compared with the wild type. (B) Comparison of the shape and size of the kidneys, hearts and spleens revealed that the $SIX1$ mutant kidneys were significantly smaller than the wild type; however, no obvious differences were observed in the hearts and spleens

of the $SIX1$ mutant and the wild-type foetuses. HE staining revealed no obvious differences between the $SIX1$ mutant and the wild-type organs (Figure S1). Taken together, these results demonstrate that deletion of $SIX1$ gene resulted in abnormal kidney development in the porcine foetus.

3.3 | The branching morphogenesis of the ureteric bud was incomplete in the $SIX1^{-/-}$ porcine foetus

The formation of a permanent kidney occurs via the interaction between the MM and the UB. The UB, a branching epithelial tube originating from the Wolffian duct, invades into the MM and then grows and branches to induce the interaction. It branches in a highly reproducible way and induces nephron formation at each of tips. Thus, the branching of the UB is critical for normal renal development. We previously determined that knockout of the $SIX1$

gene caused hypoplasia of the ureter in the $SIX1^{-/-}$ pig foetuses. We therefore investigated whether $SIX1$ mutation had an effect on the development of the UB in the porcine kidney by analysing the expressions of PAX8, PAX2 and E-cadherin. PAX8 and PAX2 are known to be expressed in the nephric tubules and the collecting duct. E-cadherin is the epithelial cell adhesion molecule that links the actin cytoskeleton to adjacent cells to form epithelial tissues. The immunohistochemistry images of PAX8 and E-cadherin in wild-type kidney tissues indicated an apparent branching morphogenesis and formation of a large number of collecting tubules derived from the UB and elongating from the medulla to the cortex. By contrast, this branching morphogenesis was not apparent in the $SIX1^{-/-}$ kidney, which also had few collecting tubes (Figure 7A). Western blots showed that the expression level of PAX2 was lower in the $SIX1$ mutant kidney than in the wild type (Figure 7B,C). Thus, these results suggest that $SIX1$ mutation can affect the development of the UB and cause the failure of branching morphogenesis of the UB.

3.4 | The expression of metanephric regulators in $SIX1$-deficient pigs

SALL1 and SIX2 are expressed in nephron progenitors as well as in differentiating nascent nephrons. SALL1 maintains nephron progenitors and nascent nephrons,[32] while SIX2 regulates nephronic progenitor self-renewal, suppresses epithelial differentiation and promotes maintenance of the MM. During the process of kidney maturation, nephron progenitors also continue to differentiate and to decrease in number. We used IHC to show the degree of differentiation of nephron progenitors by their expression of SALL1 and SIX2 (Figure 8A,B). The expression levels of SALL1 and SIX2 were significantly increased in the $SIX1$-deficient kidney than in the wild-type counterpart, indicating an apparent developmental delay in the differentiation of nephron progenitors and thus, a potential suppression of the interactions between the MM and the UB.

Previous studies have shown that EYA1, SIX1 and PAX2 interact in a molecular pathway to regulate the mesenchymal production of GDNF during UB growth and branching. A requirement for SIX1 was already indicated for the expression of PAX2 in the kidney of the $SIX1^{-/-}$ pig foetuses (Figure 7B,C), so a SIX1-PAX2 pathway appeared to operate during metanephros in the developing pig foetuses. EYA1 expression was unaffected in the metanephric mesenchyme of the $SIX1^{-/-}$ mice. We examined whether the expression of EYA1 was altered in the $SIX1$-deficient porcine kidney by IHC (Figure 8A,B) and Western blotting (Figure 8C,D), and we found that the EYA1 expression was significantly increased when compared to expression in the wild-type pigs. This indicated that the knockout of the $SIX1$ gene might increase the expression of EYA1 by some type of regulation. Previous studies have identified a requirement for SIX1 for spatial restriction of BMP4 activity in the mesenchyme surrounding the nascent UB. The genetic lowering of BMP4 activity in $SIX1^{-/-}$ mice restored UB branching and kidney
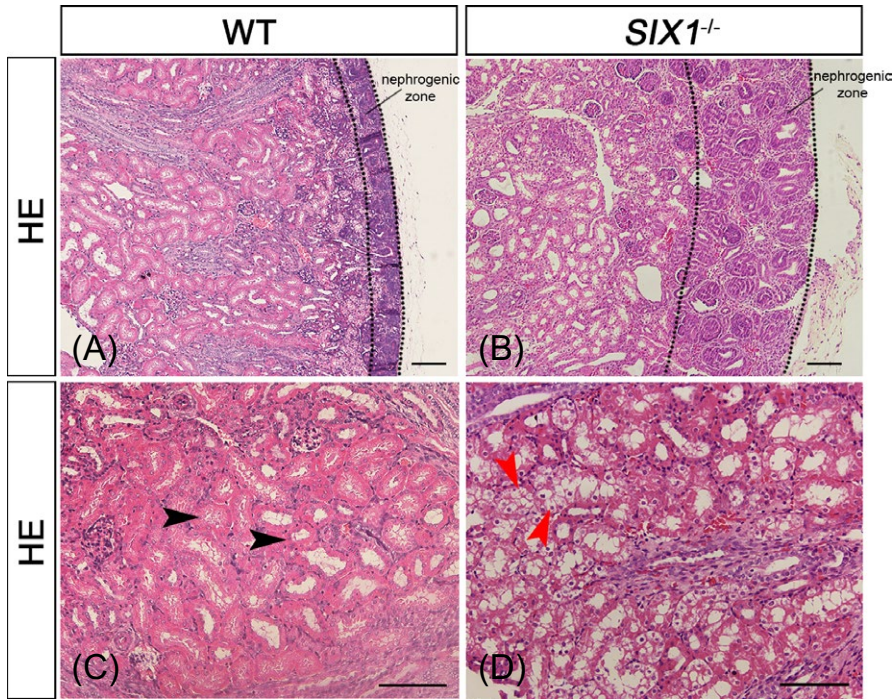
FIGURE 5 Haematoxylin and eosin (H&E) stained of wild-type and $SIX1^{-/-}$ porcine foetuses. (A, B) Glomeruli, tubules, comma-shaped bodies and S-shaped bodies are present in kidneys of both SIX1-deficient and wild-type porcine foetuses. However, the nephrogenic zone (dashed line) was markedly widened in the $SIX1^{-/-}$ kidney. (C, D) Renal tubules of SIX1-deficient kidney appeared to be undergoing vacuolar degeneration (red arrows) when compared with wild-type counterparts (black arrows). Bars = 100 μm

organogenesis in vivo. In the present study, IHC (Figure 8A,B) and Western blotting (Figure 8C,D) showed that the expression of BMP4 was still reduced in the mesenchyme of the SIX1-deficient porcine kidney, indicating that other factors or other mechanisms might restrict BMP4 activity.

3.5 | The expression of metanephric regulators in SIX1-deficient PK15 cells

To obtain SIX1 knockout PK15 cell lines, we co-transfected the Cas9-sgRNA1 vector and the TD-tomato plasmid into PK15 cells, followed by selection with G418 for approximately 8 days. 55 single-cell-derived cell colonies were collected and analysed. Genotyping analysis indicated that #49 PK15 cells were biallelic mutant (Figure 9A) and were used for the subsequent experiments.

We further investigated the interaction of metanephric signalling pathways via evaluating the expression of the metanephric regulators PAX2, PAX8, SALL1 and E-cadherin by Western blotting and quantitative analysis. The transcription factors PAX2 and PAX8, which are co-expressed in nephric duct precursors, are central regulators of kidney development.[21] Consistent with our results in the $SIX1^{-/-}$ porcine kidney, PAX2 and PAX8 were weakly expressed in $SIX1^{-/-}$ PK15 cells when compared to wild-type controls (Figure 9B,C), suggesting that PAX2 and PAX8 are essential regulators of porcine kidney organogenesis and might act as downstream regulators of the SIX1 protein.

SALL1 is also expressed in the metanephric mesenchyme,[24] and its absence increased apoptosis of the MM.[33] In the present study, SALL1 expression increased in the SIX1 mutant PK15 cells (Figure 9B,C) and this increased expression of SALL1 in the $SIX1^{-/-}$ PK15 cells coincided with its expression in the SIX1-deficient pig

foetuses. This indicates a possible increase in the number of nephron progenitors.

E-cadherin is a major protein marker of the epithelial-mesenchymal transition (EMT). A marked decrease in E-cadherin protein expression might have resulted in a blockade of the differentiation of nephron progenitors into epithelial cells (Figure 9B,C).

3.6 | Kidney phenotypic characterization of $SIX1^{-/-}SIX4^{-/-}$ porcine foetuses

We used HE staining of kidney tissues to determine whether the kidney phenotypes were disrupted in SIX1/SIX4-deficient pig foetuses. The wild-type foetuses showed a normal size and morphology for the kidney (Figure 10A), whereas the kidney of SIX1/SIX4-deficient pig foetus (#1), even though they had a similar body length, showed severely retarded development and failed to develop mature kidneys (Figure 10B,C). When compared with the mature appearance of the wild-type kidney (Figure 10A), the SIX1/SIX4-deficient kidney remained at an early stage of initial metanephros formation, where the ureteric bud had invaded into the MM and branched to generate a T-like structure (Figure 10B,C). We also found glomeruli, tubules and ureters in the wild-type kidney (Figure 10A, red arrows), but not in the SIX1/SIX4-deficient kidney (Figure 10B,C). HE staining of serial sections of tissue from the whole foetuses also revealed significantly retarded development and no recognizable kidney structures in the rest of SIX1/SIX4-deficient foetuses (Figure S2). Taken together, the results demonstrated that the disruption of both the SIX1 and SIX4 genes in the pig could cause failure of kidney development and affect foetal development as a whole (Figure 10).
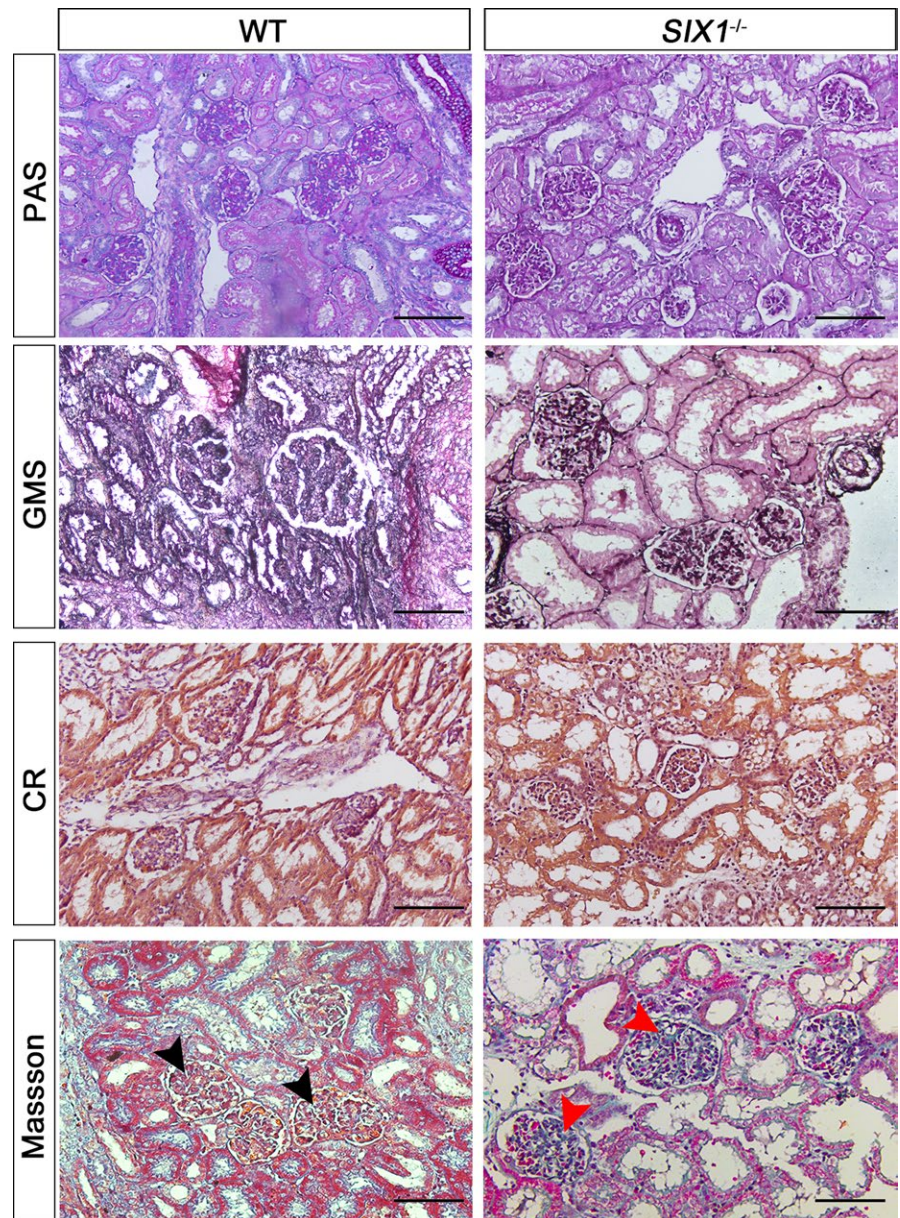
FIGURE 6 Periodic acid-Schiff (PAS), Grocott's methenamine-silver (GMS), Congo red (CR) and Masson's trichrome staining of the kidney of wild-type and $SIX1^{-/-}$ porcine foetuses. No significant differences were noted in the kidneys following PAS, GMS and CR staining. However, Masson's trichrome staining revealed a significant increase in glomerular collagen fibres (red arrows) in the kidneys of the $SIX1^{-/-}$ porcine foetuses when compared to the wild type (black arrows). Bars = 100 μm

We also found that the sizes of the testis (Figure 10B) and heart (Figure 11B) were smaller in E36 $SIX1/SIX4$-deficient pig foetuses than in the wild type (Figures 10A and 11A). However, unlike the kidneys of the $SIX1/SIX4$-deficient pig foetuses, the E36 testis and heart and E45 heart (Figure 11C) had similar internal anatomical structures when compared with the wild type. We therefore infer that the disruption of both $SIX1$ and $SIX4$ genes in the pig might affect the organ development, especial kidney development, and caused subsequent foetal lethality.

3.7 | Off-target analysis

A certain degree of off-target cutting of the CRISPR/Cas9 system has been reported in some studies. Therefore, we attempted to test the possible off-target effects in $SIX1^{-/-}$ and $SIX1^{-/-}/SIX4^{-/-}$ foetuses. 36 and 34 potential OTSs for sgRNA1 and sgRNA4 were predicted by online software, respectively. 20 higher scores OTSs (Table S1.) were PCR amplified using genomic DNA isolated from $SIX1^{-/-}$ and $SIX1^{-/-}/SIX4^{-/-}$ foetuses and WT controls. Primers for amplifying the off-target sites are listed in Table S2. Sanger sequencing of the PCR products indicated that none of the sequencing reads had mutation, suggesting that no off-target occurred at these sites in the $SIX1^{-/-}$ and $SIX1^{-/-}/SIX4^{-/-}$ foetuses.

4 | DISCUSSION

One of the ultimate goals of regenerative medicine is to generate patient-specific organs using patient-specific pluripotent stem cells. Interspecies blastocyst complementation provides an alternative approach; however, the hosts suitable for the study of kidney regeneration are mainly rodents.[4] Until now, large
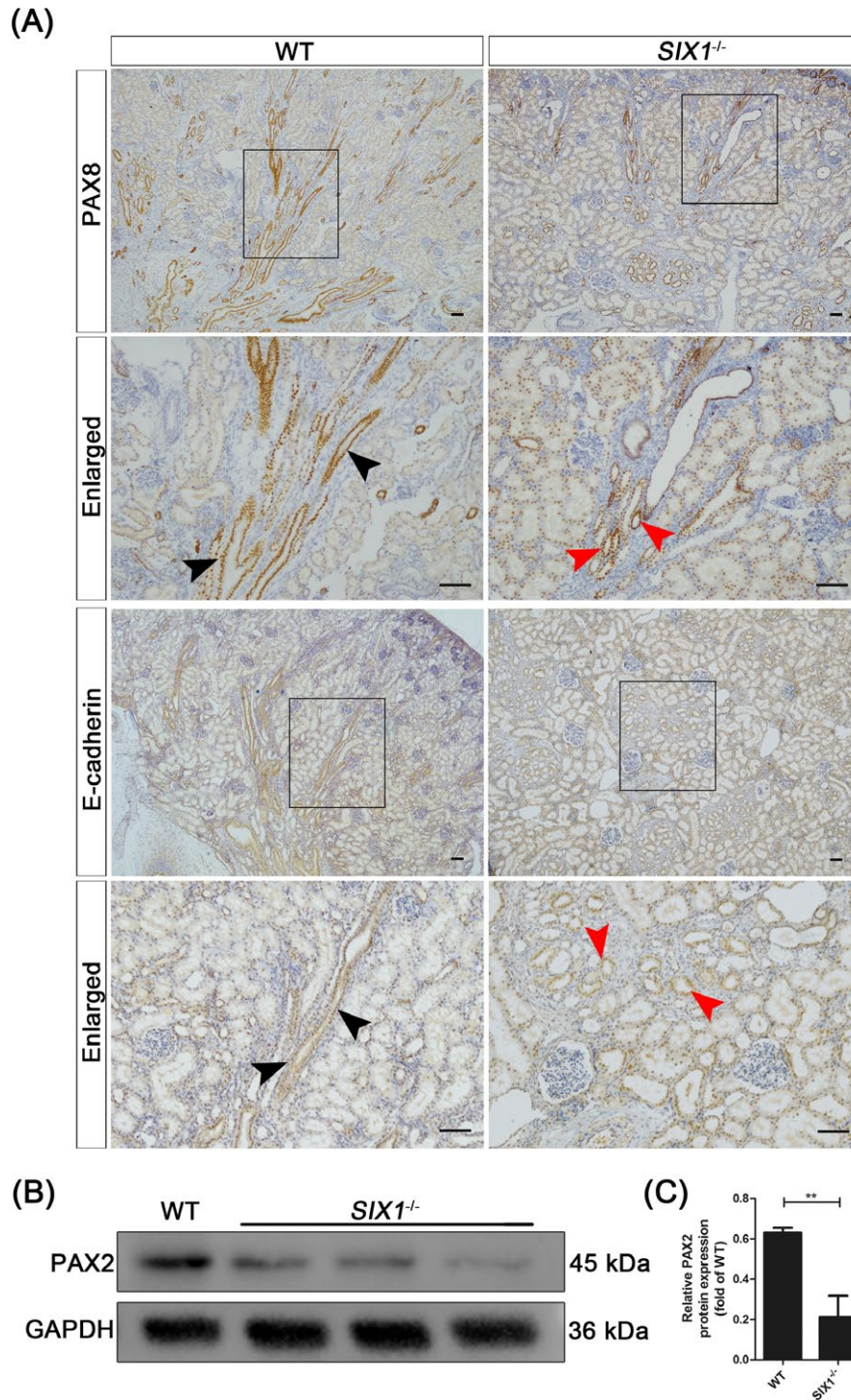
FIGURE 7 UB branching morphogenesis is incomplete in *SIX1*-deficient embryos. (A) Representative immunohistochemical images of PAX8 and E-cadherin showing that the branching morphogenesis of UB was incomplete in the kidneys of *SIX1$^{-/-}$* porcine foetuses compare with wild-type kidneys. Western blotting analyses (B) and quantitative analysis (C) show a decrease in PAX2 protein expression, indicating an apparent branching morphogenesis and formation of a large number of collecting tubules (black arrows). By contrast, this branching morphogenesis was not apparent in the *SIX1*-deficient kidney (red arrows). **$P < 0.001$. Bars = 100 μm

animals with similar anatomy, size and physiology to humans but lacking the ability to generate kidney organs have not been available. Previous studies have shown that CRISPR/Cas9 can be successfully used to generate target mutations in pigs.[30,34-36] Here, we efficiently disrupted the *SIX1* and *SIX4* genes in pigs by altering the protein coding sequence, and we demonstrated that both *SIX1* and *SIX4* gene knockout in pig foetuses result in disruption of their nephrogenesis phenotype, thereby providing an empty organ niche for the potential generation of human kidneys in pigs.
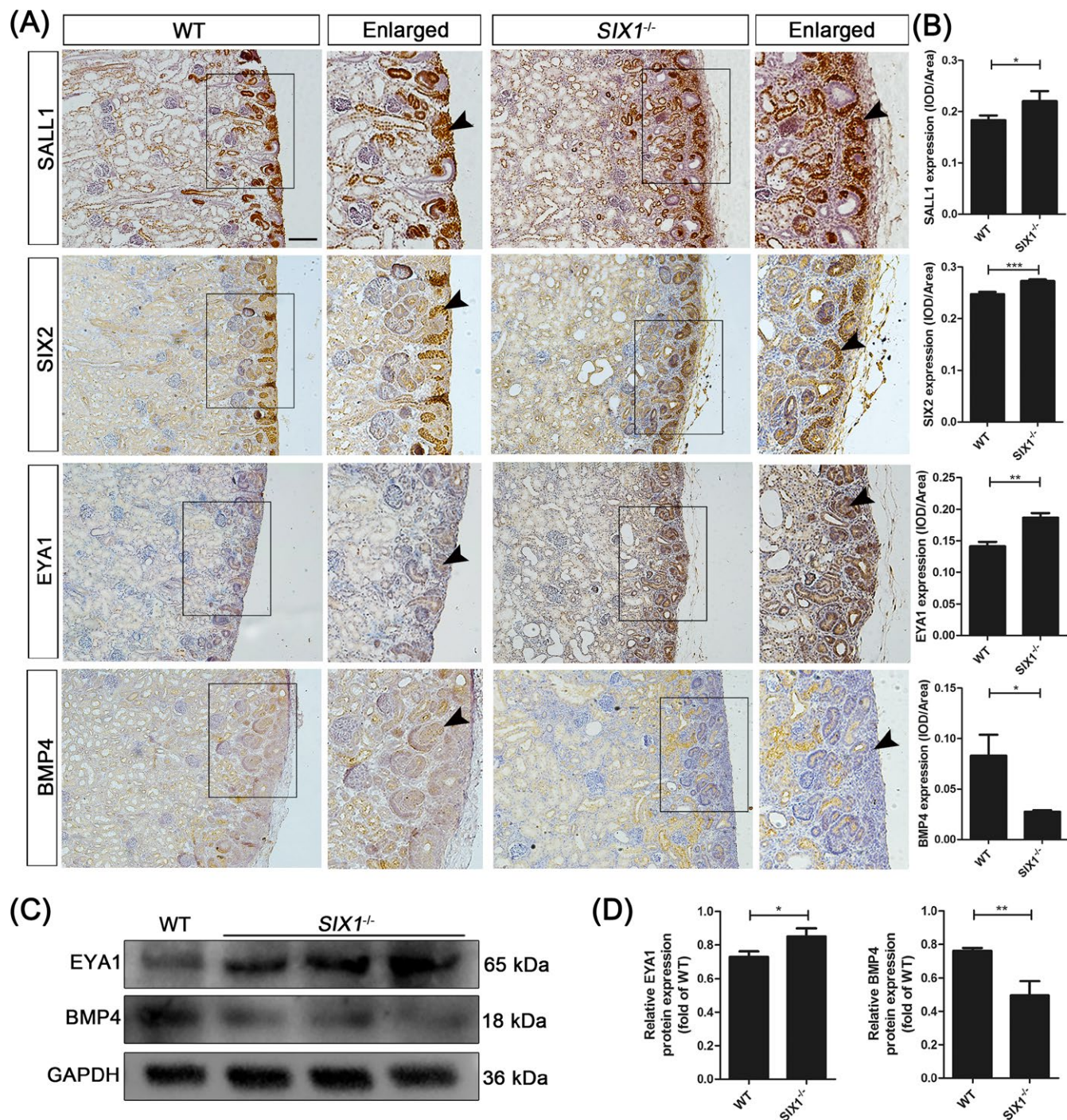
FIGURE 8 Expression of SALL1, SIX2, EYA1 and BMP4 in kidney tissue. A, Representative immunohistochemical images of the nephrogenic zone (black arrows) demonstrates upregulation of SALL1, SIX2 and EYA1, and downregulation of BMP4 in the kidneys of the $SIX1^{-/-}$ pig when compared with the wild type. B, Semi-quantitative evaluation of SALL1, SIX2, EYA1 and BMP4 expression is represented as the IOD/Area (n = 3). C, Western blotting depicting protein levels of EYA1 and BMP4 in kidney tissues. D, The $SIX1^{-/-}$ group showed a significant increase in EYA1 and a decrease in BMP4 expression. Each bar represents means ± SD. *$P < 0.05$; **$P < 0.001$; ***$P < 0.0001$. The scale bar is 100 μm

The process of kidney development is successive and complex, and the interaction between the ureteric bud and the metanephric mesenchyme is important for kidney development. During these interactions, the UB undergoes a complex branching morphogenesis to give rise to the urinary collecting duct system, while the metanephric mesenchyme ultimately forms the nephrons and the interstitial tissue of the kidney.[7] In this paper, we demonstrated that the UB grows out normally and elongates to differentiate into a ureter but fails to form a complete collecting system in $SIX1$-deficient pig foetuses, a finding that is consistent with the previous

(A)

SIX1 TCGATGCT**GCCATCGTTCGGCTTCACAC**<u>AGG</u>AGCAAGTGGCTTGCGTGTGCGAGGTTCT (WT)

#49 TCGATGCTGCCATCGTTCGGCTTC**A**ACACAGGAGCAAGTGGCTTGCGTGTGCGAGGTTCT (+1)

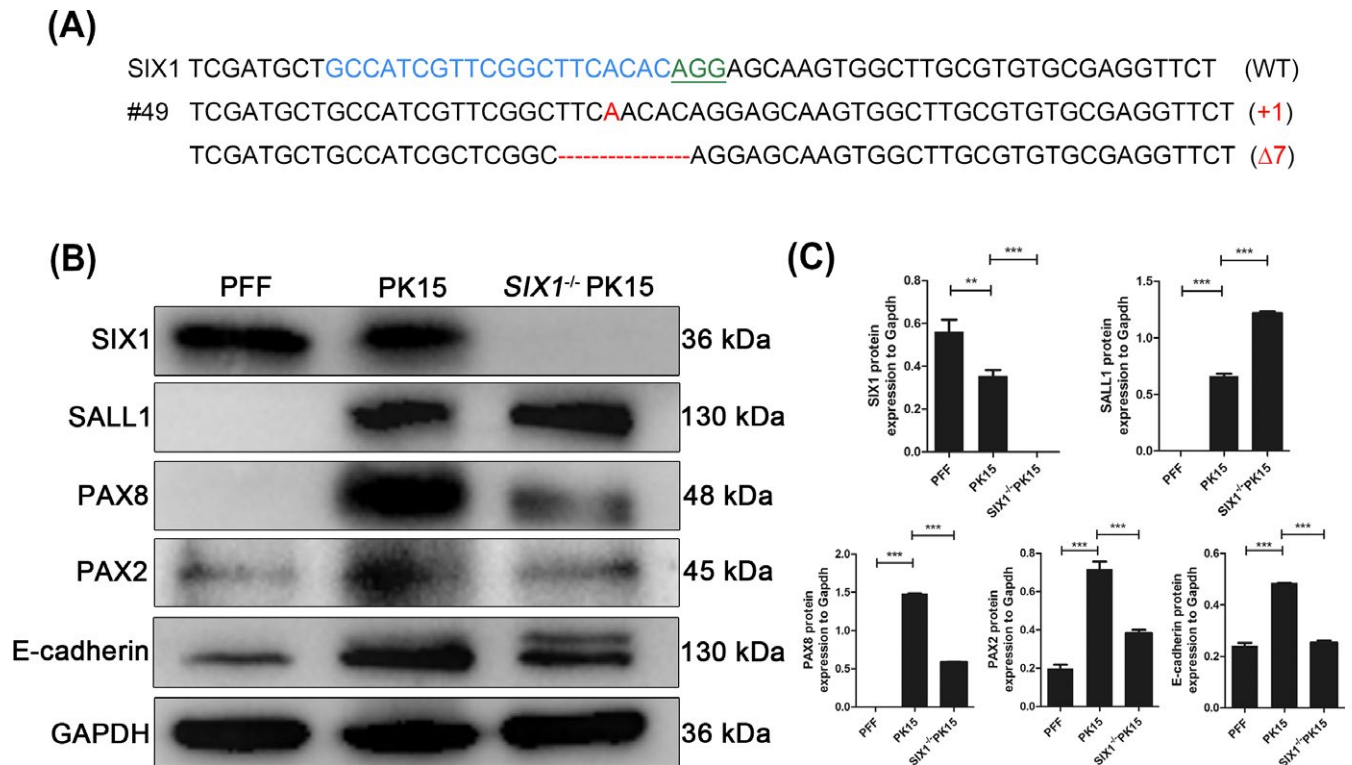TCGATGCTGCCATCGCTCGGC----------------AGGAGCAAGTGGCTTGCGTGTGCGAGGTTCT (Δ7)

FIGURE 9 Expression of SIX1, SALL1, PAX8, PAX2 and E-cadherin in PK15 cells. (A) Sequences of the targeting sites in mutant colonies. Western blotting analyses (B) and quantitative analyses (C) showed higher expression levels of SALL1 and lower expression levels of PAX8, PAX2 and E-cadherin in $SIX1^{-/-}$ PK15 cells compared to wild-type PK15 cells and PFFs. SIX1 protein was not detectable in $SIX1^{-/-}$ PK15 cells. PFFs, porcine foetal fibroblasts. Data are depicted as mean ± SD. **$P < 0.001$. ***$P < 0.0001$. The sgRNA sequences are highlighted in blue, PAM sequences in green, and insertions in red; deletion (Δ); insertion (+)
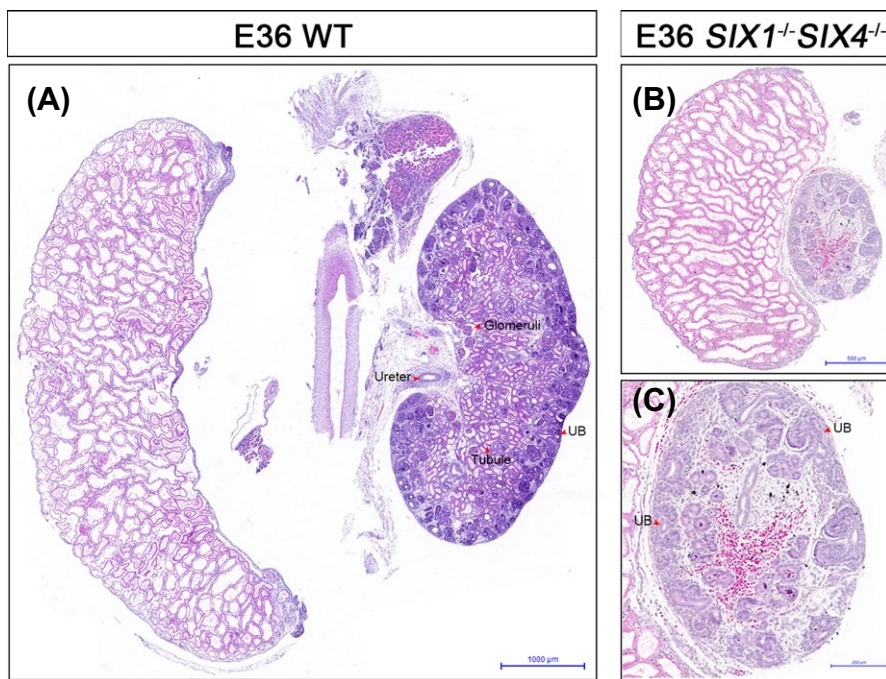

FIGURE 10 Overall view of the kidney of wild-type and $SIX1^{-/-}/SIX4^{-/-}$ porcine foetuses at embryonic day 36 (E36). The kidney of $SIX1/SIX4$-deficient pig foetuses was severely retarded and remained at the early stage of initial metanephros formation (B, C) compared with the mature appearance of wild-type kidney (A). Bars = 1000 μm in (A), 500 μm in (B), 200 μm in (C)

studies in mice. The failure to form mature collecting ducts may be caused by the inhibition of GDNF and the formation of ectopic UBs. GDNF is a key regulator of UB outgrowth, branching and generation of the metanephric collecting duct system.[37,38] The maintenance and/or activation of GDNF expression in the MM depends on a number of regulatory factors, including SIX1, SIX4,
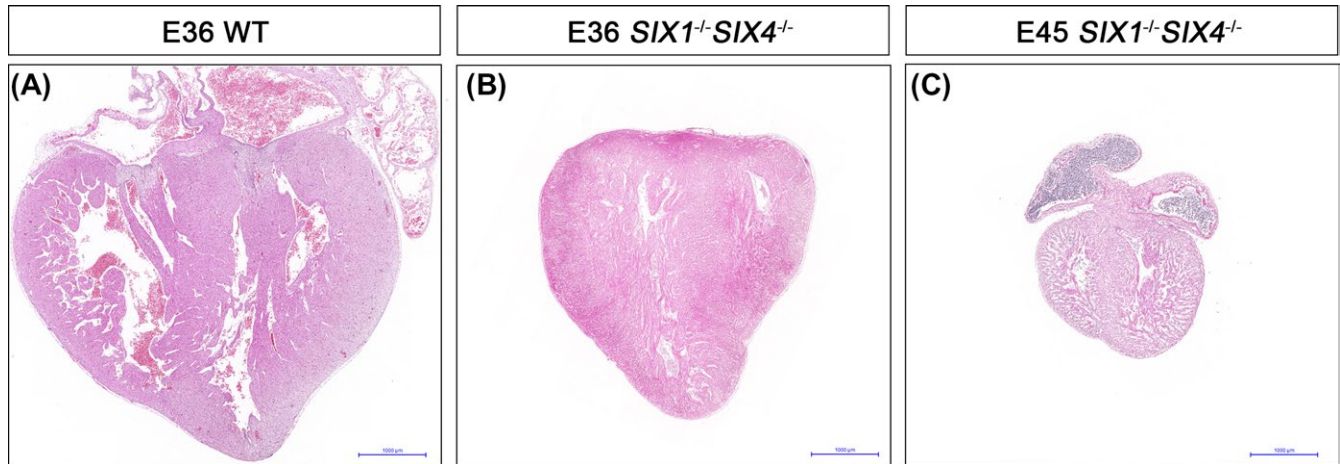
FIGURE 11 Overall view of the heart of wild-type and *SIX1*^{-/-} porcine foetuses. Haematoxylin-eosin staining shows as smaller size for the hearts of *SIX1/SIX4*-deficient pig foetuses (B, C) than for the wild type (A); however, the internal anatomical structures are similar. Bars = 1000 μm

PAX2 and PAX8. Downregulation of PAX2 and PAX8 expression in *SIX1*^{-/-} foetuses and *SIX1*^{-/-} PK15 cells suggests that the *PAX2* and *PAX8* genes may be the downstream targets of the SIX1 protein. *SIX1* mutation may therefore suppress GDNF expression indirectly by regulating the expression of PAX2 and PAX8. In addition, the observations made by Xu et al[18] suggest the existence of an EYA1-Six-PAX2 regulatory hierarchy that controls early kidney development in mice. However, EYA1 expression is increased in the early kidney development of *SIX1*-deficient pig foetuses. These findings indicate that a feedback regulation might exist between EYA1 and SIX1/PAX2, so that the decrease in SIX1 and PAX2 expression might activate EYA1 expression.

BMP4 is a negative regulator of UB outgrowth and is expressed in the stromal cells surrounding the nephric duct prior to UB outgrowth.[39] *BMP4* null embryos die during early kidney development, whereas heterozygotes display ectopic or duplicated UBs.[40] Thus, the impaired formation of collecting ducts in *SIX1*^{-/-} porcine foetuses may result from the production of ectopic and duplicated UBs caused by the reduction in BMP4 expression.

The cap mesenchyme undergoes a mesenchyme-to-epithelial transition (MET) to form renal vesicles and then elongates into an S-shaped body that fuses with the collecting duct epithelium.[9,41] SIX2 and SALL1 are important for the self-renewal of the progenitor population and regulating the process of MET.[42] Furthermore, *SIX2*-deficient mice undergo exuberant MET.[43] Our immunohistochemistry data showed that the upregulation of SIX2 and SALL1 expression increased the number of nephron progenitors in *SIX1*-deficient foetuses compared with the wild type, suggesting that MET might be blocked and that differentiation of progenitors might be delayed. The downregulated expression of E-cadherin showed the decreased number of epithelial cells, which further confirmed the block of MET and the possible inhibition of the interactions between the MM and the UB. Taken together, our data support the idea that SIX1 is a crucial regulator of early-stage kidney development and that *SIX1* mutants fail to form a complete collecting system.

The kidney of the *SIX1/SIX4*-deficient pig foetus exhibited a more severely disrupted kidney phenotype than did the *SIX1*-deficient pig foetus, which is consistent with the observations in mice. Compared to wild-type controls, the ureters and bilateral kidneys failed to develop in the *SIX1/SIX4*-deficient pig foetus. The *SIX1/SIX4*-deficient mice died soon after birth and showed developmental defects in various organs.[44] We also found the mutation of *SIX1/SIX4* genes caused embryonic lethality. This demonstrated that the SIX1 and SIX4 homeoproteins are required for the development of the mammalian embryo.

In humans, the mutation of *SIX1* causes branchio-oto-renal (BOR) syndrome,[45] an autosomal-dominant disorder characterized by hearing loss and branchial and renal anomalies.[46] In our pig study, we found that *SIX1* deficiency can cause various kidney defects and ear deformities. Therefore, the *SIX1*-deficient pig foetus may be useful for elucidating the mechanism underlying this type of disease.

In summary, we successfully generated *SIX1* and *SIX1/SIX4* targeted pig foetuses using the CRISPR/Cas9 system combined with somatic cell nuclear transfer (SCNT) technology. Our study demonstrated that *SIX1* is required for the UB growth and branching occurring during early kidney development. As in other species, suppression of *SIX1* and *SIX4* gene expression in the pig foetus led to the disruption of kidney development.

ORCID

Manling Liu https://orcid.org/0000-0002-9500-7728

REFERENCES

1. Jha V, Garcia-Garcia G, Iseki K, et al. Chronic kidney disease: global dimension and perspectives. *Lancet*. 2013;382(9888):260-272.

2. Rashid T, Kobayashi T, Nakauchi H. Revisiting the flight of Icarus: making human organs from PSCs with large animal chimeras. *Cell Stem Cell*. 2014;15(4):406-409.

3. Kobayashi T, Yamaguchi T, Hamanaka S, et al. Generation of rat pancreas in mouse by interspecific blastocyst injection of pluripotent stem cells. *Cell*. 2010;142(5):787-799.

4. Usui J, Kobayashi T, Yamaguchi T, Knisely AS, Nishinakamura R, Nakauchi H. Generation of kidney from pluripotent stem cells via blastocyst complementation. *Am J Pathol*. 2012;180(6):2417-2426.

5. Yamaguchi T, Sato H, Kato-Itoh M, et al. Interspecies organogenesis generates autologous functional islets. *Nature*. 2017;542(7640):191-196.

6. Wu J, Platero-Luengo A, Sakurai M, et al. Chimerism with mammalian pluripotent stem cells. *Cell*. 2017;168(3):473-486 e415.

7. Little MH, McMahon AP. Mammalian kidney development: principles, progress, and projections. *Cold Spring Harb Perspect Biol*. 2012;4(5):a008300.

8. Kuure S, Vuolteenaho R, Vainio S. Kidney morphogenesis: cellular and molecular regulation. *Mech Dev*. 2000;92(1):31-45.

9. Vetter MR, Gibley CW Jr. Morphogenesis and histochemistry of the developing mouse kidney. *J Morphol*. 1966;120(2):135-155.

10. Bard JB, Gordon A, Sharp L, Sellers WI. Early nephron formation in the developing mouse kidney. *J Anat*. 2001;199(Pt 4):385-392.

11. Poladia DP, Kish K, Kutay B, et al. Role of fibroblast growth factor receptors 1 and 2 in the metanephric mesenchyme. *Dev Biol*. 2006;291(2):325-339.

12. Schmidt-Ott KM, Yang J, Chen X, et al. Novel regulators of kidney development from the tips of the ureteric bud. *J Am Soc Nephrol*. 2005;16(7):1993-2002.

13. Dressler GR. Epigenetics, development, and the kidney. *J Am Soc Nephrol*. 2008;19(11):2060-2067.

14. Costantini F, Kopan R. Patterning a complex organ: branching morphogenesis and nephron segmentation in kidney development. *Dev Cell*. 2010;18(5):698-712.

15. Boyle S, Misfeldt A, Chandler KJ, et al. Fate mapping using Cited1-CreERT2 mice demonstrates that the cap mesenchyme contains self-renewing progenitor cells and gives rise exclusively to nephronic epithelia. *Dev Biol*. 2008;313(1):234-245.

16. Faa G, Gerosa C, Fanni D, et al. Morphogenesis and molecular mechanisms involved in human kidney development. *J Cell Physiol*. 2012;227(3):1257-1268.

17. Kawakami K, Sato S, Ozaki H, Ikeda K. Six family genes–structure and function as transcription factors and their roles in development. *BioEssays*. 2000;22(7):616-626.

18. Xu PX, Zheng W, Huang L, Maire P, Laclef C, Silvius D. Six1 is required for the early organogenesis of mammalian kidney. *Development*. 2003;130(14):3085-3094.

19. Nie X, Sun J, Gordon RE, Cai CL, Xu PX. SIX1 acts synergistically with TBX18 in mediating ureteral smooth muscle formation. *Development*. 2010;137(5):755-765.

20. Kobayashi H, Kawakami K, Asashima M, Nishinakamura R. Six1 and Six4 are essential for Gdnf expression in the metanephric mesenchyme and ureteric bud formation, while Six1 deficiency alone causes mesonephric-tubule defects. *Mech Dev*. 2007;124(4):290-303.

21. Krause M, Rak-Raszewska A, Pietila I, Quaggin SE, Vainio S. Signaling during kidney development. *Cells*. 2015;4(2):112-132.

22. Narlis M, Grote D, Gaitan Y, Boualia SK, Bouchard M. Pax2 and pax8 regulate branching morphogenesis and nephron differentiation in the developing kidney. *J Am Soc Nephrol*. 2007;18(4):1121-1129.

23. Sajithlal G, Zou D, Silvius D, Xu PX. Eya 1 acts as a critical regulator for specifying the metanephric mesenchyme. *Dev Biol*. 2005;284(2):323-336.

24. Kanda S, Tanigawa S, Ohmori T, et al. Sall1 maintains nephron progenitors and nascent nephrons by acting as both an activator and a repressor. *J Am Soc Nephrol*. 2014;25(11):2584-2595.

25. Bracken CM, Mizeracka K, McLaughlin KA. Patterning the embryonic kidney: BMP signaling mediates the differentiation of the pronephric tubules and duct in *Xenopus laevis*. *Dev Dyn*. 2008;237(1):132-144.

26. Godin RE, Robertson EJ, Dudley AT. Role of BMP family members during kidney development. *Int J Dev Biol*. 1999;43(5):405-411.

27. Hsu PD, Lander ES, Zhang F. Development and applications of CRISPR-Cas9 for genome engineering. *Cell*. 2014;157(6):1262-1278.

28. Li HP, Chen PG, Liu FT, et al. Characterization and anti-inflammation role of swine IFITM3 gene. *Oncotarget*. 2017;8(43):73579-73589.

29. Yang L, Guell M, Niu D, et al. Genome-wide inactivation of porcine endogenous retroviruses (PERVs). *Science*. 2015;350(6264):1101-1104.

30. Chen F, Wang Y, Yuan Y, et al. Generation of B cell-deficient pigs by highly efficient CRISPR/Cas9-mediated gene targeting. *J Genet Genomics*. 2015;42(8):437-444.

31. Dai Y, Vaught TD, Boone J, et al. Targeted disruption of the alpha1,3-galactosyltransferase gene in cloned pigs. *Nat Biotechnol*. 2002;20(3):251-255.

32. Nishinakamura R, Osafune K. Essential roles of Sall family genes in kidney development. *J Physiol Sci*. 2006;56(2):131-136.

33. Sakaki-Yumoto M, Kobayashi C, Sato A, et al. The murine homolog of SALL4, a causative gene in Okihiro syndrome, is essential for embryonic stem cell proliferation, and cooperates with Sall1 in anorectal, heart, brain and kidney development. *Development*. 2006;133(15):3005-3013.

34. Zhang W, Wang G, Wang Y, et al. Generation of complement protein C3 deficient pigs by CRISPR/Cas9-mediated gene targeting. *Sci Rep*. 2017;7(1):5009.

35. Li Z, Yang HY, Wang Y, et al. Generation of tryptophan hydroxylase 2 gene knockout pigs by CRISPR/Cas9-mediated gene targeting. *J Biomed Res*. 2017;31(5):445-452.

36. Zhang R, Wang Y, Chen L, et al. Reducing immunoreactivity of porcine bioprosthetic heart valves by genetically-deleting three major glycan antigens, GGTA1/beta4GalNT2/CMAH. *Acta Biomater*. 2018;72:196-205.

37. Costantini F, Shakya R. GDNF/Ret signaling and the development of the kidney. *BioEssays*. 2006;28(2):117-127.

38. Moore MW, Klein RD, Farinas I, et al. Renal and neuronal abnormalities in mice lacking GDNF. *Nature*. 1996;382(6586):76-79.

39. Miyazaki Y, Oshima K, Fogo A, Hogan BL, Ichikawa I. Bone morphogenetic protein 4 regulates the budding site and elongation of the mouse ureter. *J Clin Investig*. 2000;105(7):863-873.

40. Cain JE, Bertram JF. Ureteric branching morphogenesis in BMP4 heterozygous mutant mice. *J Anat*. 2006;209(6):745-755.

41. Pole RJ, Qi BQ, Beasley SW. Patterns of apoptosis during degeneration of the pronephros and mesonephros. *J Urol*. 2002;167(1):269-271.

42. Brophy PD, Ostrom L, Lang KM, Dressler GR. Regulation of ureteric bud outgrowth by Pax2-dependent activation of the glial derived neurotrophic factor gene. *Development*. 2001;128(23):4747-4756.

43. Self M, Lagutin OV, Bowling B, et al. Six2 is required for suppression of nephrogenesis and progenitor renewal in the developing kidney. *EMBO J*. 2006;25(21):5214-5228.

44. Grifone R, Demignon J, Houbron C, et al. Six1 and Six4 homeoproteins are required for Pax3 and Mrf expression during myogenesis in the mouse embryo. *Development*. 2005;132(9):2235-2249.

45. Ito T, Noguchi Y, Yashima T, Kitamura K. SIX1 mutation associated with enlargement of the vestibular aqueduct in a patient with branchio-oto syndrome. *Laryngoscope*. 2006;116(5):796-799.

46. Melnick M, Bixler D, Silk K, Yune H, Nance WE. Autosomal dominant branchiootorenal dysplasia. *Birth Defects Orig Artic Ser.* 1975;11(5):121-128.

SUPPORTING INFORMATION

Additional supporting information may be found online in the Supporting Information section at the end of the article.